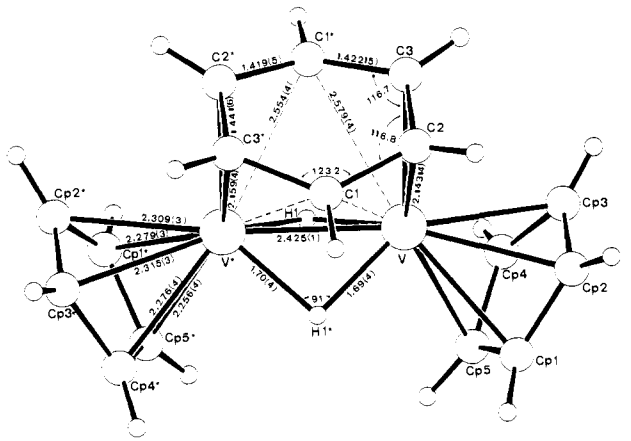

Figure 1.

a metallocene and an alkali metal.[7] Reaction of this deep red compound with 1,3-cyclohexadiene in tetrahydrofuran (THF) yields diamagnetic **1** (dark brown plates, 40%; $M^+ = 312$, ν_{VH_2V} (KBr) 1795, 1701, and 1611 cm^{-1}).

$$2K[Cp_2V] + 1,3\text{-}C_6H_8 \xrightarrow[-78\ ^\circ C \rightarrow +20\ ^\circ C]{THF} \underset{\mathbf{1}}{(CpVH)_2C_6H_6} + 2KCp \quad (1)$$

The structure of **1** has been determined by a single-crystal X-ray analysis[8] and is shown in Figure 1. Two Cp–V units are bridged by a nonplanar benzene ring as well as two hydrogen atoms in such a way that a 2-fold axis passes through the center of the six-membered ring and the middle of the V–V* link. All hydrogen atoms were located on a difference Fourier synthesis and have been included in the structural refinement. The vanadium distance of 2.425 (1) Å compares favorably with that found in accurate studies of $Cp_2V_2(CO)_5$[9] (2.459 (3) Å) and its triphenylphosphine derivative $Cp_2V_2(CO)_4PPh_3$ (2.466 (1) Å).[10] These compounds contain semibridging carbonyl groups, and the metal–metal bonds have been assigned multiple bonding character. A formal triple bond between two bridged vanadium atoms has been assigned for a metal–metal distance of 2.200 (2) Å in $V_2(2,6\text{-}(MeO)_2Ph)_4 \cdot THF$.[11a] Assignment of bond orders to metal–metal bonds, however, seems only to be unambiguous when no bridging groups are linking the metal–metal unit.[11b,12]

There is a noncrystallographic mirror in the plane of C1, C1*, H1, and H1* and a dihedral angle between both planar Cp rings of 69.7°. The interplanar angle in the folded benzene moiety is 19.8°. Whereas all C–C distances within this unit are equal within 3σ (av 1.427 (10) Å), the metal–carbon distances (V–C2 2.143 (4), V–C3 2.159 (4) Å) as well as the angles within the ring (C1–C2–C3 116.8 (3)°, C2–C3–C1* 116.7 (3)°, C2–C1–C3* 123.2 (3)°) are slightly different. The distances to the bridging carbon atoms are 2.554 (4) Å for V–C1 and 2.579 (4) Å for V–C1*. The hydrogen atom attached to this carbon atom is bent by 0.12 Å toward the midpoint between the vanadium atoms. The bridging hydrogen atoms are arranged symmetrically (V–H 1.70 (4), V*–H 1.69 (4) Å, V–H–V* 91 (2)°) and show a nonbonding H–H separation of 1.97 (5) Å.

1 is a fluxional molecule in solution. At −115 °C the ^1H NMR spectrum (400 MHz) of a THF-d_8 solution shows four resonances: δ 4.49 (4 H), 2.99 (2 H), 5.49 (10 H, Cp), −2.74 (2 H, bridging hydrogens). Coalescence of the first two resonances into one signal at δ 3.99 occurs at −90 °C. The chemical shift of the vanadium-bound hydrogen remains unaffected between −115 °C and room temperature although the half-width of the signal increases. The ^{13}C NMR spectrum (25.2 MHz) at room temperature shows only two signals (δ 97.9 ($^1J_{CH}$ = 173 ± 1 Hz, Cp), 76.2 ($^1J_{CH}$ = 169 ± 1 Hz, C_6H_6)). On lowering the temperature to −120 °C the signal for the C_6H_6 ring is slightly broadened ($\Delta\nu_{1/2} \approx 20$ Hz), but full coalescence is not achieved. We interpret these results as a rotation of the C_6H_6 ring about its midpoint.

Compound **1** reacts with carbon monoxide according to eq 2.

$$\underset{\mathbf{1}}{(CpVH)_2C_6H_6} + 8CO \rightarrow 2CpV(CO)_4 + 0.75C_6H_8 + 0.25C_6H_6 + 0.25H_2 \quad (2)$$

Both benzene and 1,3-cyclohexadiene are observed in the condensate of the reaction mixture. Cyclohexadiene is formed as a result of transfer of the metal-bound hydrogen to the C_6H_6 ring, while displacement of the C_6H_6 ring as benzene is accompanied by the evolution of an equimolar amount of hydrogen. Quantitative liberation of benzene and hydrogen was effected by treating **1** with iodine (eq 3). A new vanadium(II) halide is formed, which

$$\underset{\mathbf{1}}{(CpVH)_2C_6H_6} + I_2 \xrightarrow{THF} \underset{\mathbf{2}}{2[CpVI(THF)]} + C_6H_6 + H_2 \quad (3)$$

may be isolated directly as [CpVI(THF)] (**2**) or as adducts of tertiary phosphines or acetonitrile, e.g., $CpVIP_2$ [$P_2 = 2P(CH_3)_3$, diphos, or $CyPC_2H_4PCy_2$ (Cy = C_6H_{11})] or $CpVICH_3CN$.

Acknowledgment. We thank Drs. Benn and Mynott for carrying out and interpreting the NMR experiments.

Registry No. 1, 86421-59-2; **2**, 86374-51-8; $CpVI(P(CH_3)_3)_2$, 86436-05-7; CpVIdiphos, 86421-61-6; $CpVICy_2PC_2H_4PCy_2$, 86421-62-7; $CpVICH_3CN$, 86421-63-8; $K[Cp_2V]$, 86421-60-5; CO, 630-08-0; I_2, 7553-56-2; 1,3-cyclohexadiene, 592-57-4.

Supplementary Material Available: Atomic coordinates and thermal parameters for **1**, a table of selected interatomic distances and interbond angles, and a list of observed and calculated structure factors (10 pages). Ordering information is given on any current masthead page.

(7) We previously reported 1:1 adducts between alkali metals and metallocenes and between alkali metals and half-sandwich compounds, e.g., $[M(THF)_x][(C_5H_5)_2Co]$ and $[M(THF)_x][C_5H_5CoCOD]$[5] (M = Li or K, COD = 1,5-cyclooctadiene).

(8) **1** crystallizes in the orthorhombic space group *Fdd*2 (No. 43). Cell dimensions: a = 16.905 (2) Å, b = 20.977 (2) Å, c = 7.699 (1) Å, Z = 8, d_{calcd} = 1.52 g cm^{-3}, R = 0.028 (R_w = 0.036), 117 parameters refined with 1764 reflections, of which 342 were considered unobserved (2σ).

(9) Fischer, E. O.; Schneider, R. J. *Chem. Ber.* **1970**, *103*, 3648. Cotton, F. A.; Frenz, B. A.; Kruczynski, L. *J. Am. Chem. Soc.* **1973**, *95*, 951. Cotton, F. A.; Kruczynski, L.; Frenz, B. A. *J. Organomet. Chem.* **1978**, *160*, 93.

(10) Huffmann, J. C.; Lewis, L. N.; Caulton, K. G. *Inorg. Chem.* **1980**, *19*, 2755.

(11) (a) Seidel, W.; Kreisel, G.; Mennenga, H. *Z. Chem.* **1976**, *16*, 492. (b) Cotton, F. A.; Millar, M. *J. Am. Chem. Soc.* **1977**, *99*, 7886.

(12) (a) Cotton, F. A.; Walton. In "Multiple Bonds in Metal Atoms"; Wiley: New York, 1982. (b) Goddard, R.; Krüger, C. In "The Electron Distribution and the Chemical Bond"; Plenum Press: New York, 1982.

Carbene Chemistry of Cations: The Chemistry of $:C_3H^+$ in the Gas Phase

Diethard K. Bohme,* Asit B. Raksit, and Arnold Fox

Department of Chemistry and Centre for Experimental Space Science York University, Downsview, Ontario M3J 1P3, Canada

Received March 7, 1983

Much attention has been directed over the years toward the chemistry of neutral carbenes as reactive intermediates. Here we suggest and explore the notion that carbene character may be associated also with ions. We have chosen the alkynylcarbene cation, $:C_3H^+$, as our exemplary species.[1] Cationic and carbene character is indicated for this ion by the linear resonance structure (1), which has been shown by molecular orbital theory to be the

$$\overset{+}{H}\text{–}C\text{=}C\text{=}C\text{:} \leftrightarrow H\text{-}C\equiv C\text{-}C\text{:}^+ \quad (1)$$

most stable form of C_3H^+.[2] In addition to these properties, the

(1) $:C_3H^+$ may be regarded as the carbene cation derivative (by hydride abstraction) of vinylidene carbene, $H_2C\text{=}C\text{=}C\text{:}$, or propargylene, $HC\equiv C\text{—}\ddot{C}H$. Alternatively $:C_3H^+$ may be derived from the protonation at a terminal carbon of the dicarbene, $:C\text{=}C\text{=}C\text{:}$, which is the process upon which the nomenclature of this species is based.

0002-7863/83/1505-5481$01.50/0

Table I. Rate Constants and Product Distributions Measured for Reactions of C_3H^+ in the Gas Phase at 296 ± 2 K

neutral reactant[a]	products[b]	product distribution[c]	k[d]
H_2 (He)	$C_3H_3^+$	1.0	1.9 (−27)[e]
CO (He)	C_4HO^+	1.0	2.9 (−27)[e]
H_2O	$CHO^+ + C_2H_2$	0.55	4.5 (−10)
	$C_2H_3^+ + CO$	0.40	
	$C_3HO^+ + H_2$	0.05	
H_2S	$CHS^+ + C_2H_2$	0.63	1.2 (−9)
	$C_2H_3^+ + CS$	0.30	
	$C_3HS^+ + H_2$	0.07	
CO_2	$C_3HO^+ + CO$	1.0	2.0 (−12)
CH_4	$C_2H_3^+ + C_2H_2$	0.7	5.5 (−10)
	$C_3H_3^+ + CH_2$	0.2	
	$C_4H_3^+ + H_2$	0.1	
CH_3OH	$C_3HO^+ + CH_4$	0.8	2.2 (−9)
	$CH_3O^+ + C_3H_2$	0.1	
	$CH_3^+ + C_3H_2O$	0.1	
C_2H_4	$C_3H_3^+ + C_2H_2$	0.95	9.5 (−10)
	$C_5H_3^+ + H_2$	0.05	

[a] For termolecular reactions the third body is indicated in parentheses. [b] The neutral products were not detected in the present experiments. In writing the neutral product only the most exothermic channel is indicated. [c] We estimate that the absolute branching ratio may be in error by as much as ±30% due to possible mass discrimination effects in the mass spectrometer. For ionic products over a narrow mass range (≲5 amu) these effects are negligible. [d] Unless otherwise indicated, k is the bimolecular rate constant for the disappearance of C_3H^+ in units of cm^3 $molecule^{-1}$ s^{-1}. The accuracy is estimated to be better than ±30%. Rate constant are expressed as a $(-b)$ to represent $a \times 10^{-b}$. [e] Termolecular rate constant in units of cm^6 $molecule^{-2}$ s^{-1}.

high energy and low Brönsted acidity of $:C_3H^+$[2,3] make this species very attractive for exploring its carbene chemistry.[4] We have been able to generate C_3H^+ from propene in a selected ion flow tube (SIFT) mass spectrometer and to follow directly the reactions of this ion with a wide choice of neutral substrates.[5] The results of these investigations have indicated that we have produced the most stable form of C_3H^+ and that its observed chemistry is consistent with carbenoid behavior.

Table I indicates that the observed reactions of C_3H^+ in the gas phase exhibit a large variety of pathways and a wide range of reactivities. A large fraction of the observed reaction paths correspond to those usually associated with neutral carbene chemistry.[6] They include the following:

(1) Coordination with a Nucleophile Possessing a Nonbonded Electron Pair. Examples of products are found in Table I that may result from coordination with a nonbonded electron pair on oxygen as is the case with CO_2, CH_3OH, and H_2O, on sulphur as is the case with H_2S, and on carbon as is the case with CO. The reaction with CO_2 proceeds exclusively to produce HC_3O^+, which is likely to have the structure $HC^+{=}C{=}C{=}O$. This ion is also a major product in the reaction of C_3H^+ with methanol and a minor product in the corresponding reaction with H_2O. The sulphur analogue is produced with H_2S. With CO the higher member $HC^+{=}C{=}C{=}C{=}O$ of the homologous series HC_nO^+ appears to be produced exclusively.

A number of the product ions formed in these coordination reactions are of interest from the point of view of molecular synthesis. In particular, subsequent proton-transfer or hydride-abstraction reactions of the HC_nO^+ ions can establish members of the unsaturated homologous series $:C(C)_nO$ or $H_2C(C)_nO$, respectively. We shall attempt to explore these aspects further.

(2) Insertion into a σ Bond. The reactions in Table I include examples of insertions into H–H, O–H, S–H, and C–H bonds. Hydrogen was observed to add to C_3H^+ in helium buffer gas to form $C_3H_3^+$. If the reaction proceeds by *broadside* attack, formation of the propargyl cation, $HC{\equiv}C{-}CH_2^+$, is likely to be preferred initially over the formation of the more stable cyclopropenium ion. Insertion into the other X–H bonds may proceed in a similar fashion. Formation of a propargyl-like cation followed by isomerization to a cyclic structure can lead to subsequent decomposition into C_2H_2 and an ion of the type $:CX^+$ as is indicated by reaction 2.[7] This route is endothermic for X = H but

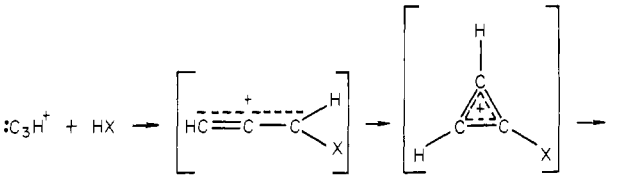

$$C_2H_2 + :CX^+ \qquad (2)$$

exothermic for X = OH, SH, and CH_3. Insertion into the O–H bond in the manner indicated by reaction 2 can account for the predominant path with H_2O to produce CHO^+ as well as the path leading to $C_2H_3^+$ if proton transfer proceeds before the products separate. An entirely analogous situation is implied by the results obtained for the reaction with H_2S. Insertion into the C–H bond in a similar fashion can account for the major product ion, $C_2H_3^+$, observed with methane.

(3) Addition to Double Bonds. The major ion product observed for the reaction with ethylene was $C_3H_3^+$ with probable elimination of C_2H_2. One possible carbenoid mechanism for this reaction would involve formation of the cyclic intermediate shown in (3)

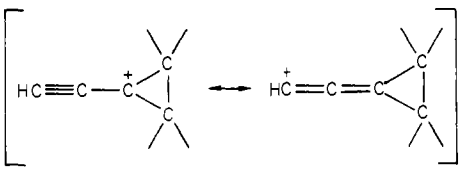

(3)

which is of the type often invoked in neutral carbene chemistry, e.g., in the chemistry of $:C{=}C{=}C:$,[8] but there is some uncertainty about the mechanism for the subsequent breakup of this ion into $C_3H_3^+$ and C_2H_2. Alternatively the reaction may proceed by carbenoid C–H bond insertion in the manner described earlier by mechanism 2.

(2) The linear form has an energy calculated to be 52.7 kcal mol^{-1} lower than that of the nonlinear form with C_{2v} symmetry (Raghavachari, K.; Whiteside, R. A.; Pople, J. A.; Schleyer, P. V. R. *J. Am. Chem. Soc.* **1981**, *103*, 5649).

(3) Bracketing experiments with ion–molecule reactions have established a heat of formation for the C_3H^+ produced in our SIFT mass spectrometer of 383 ± 8 kcal mol^{-1} (Rakshit, A. B.; Bohme, D. K. *Int. J. Mass Spectrom. Ion Phys.* **1983**, *49*, 275). The heat of formation is in agreement with that predicted in ref 2 for the linear carbene cation shown in (1). Also there is agreement with the most recent experimental investigations by: Parr, A. C.; Jason, A. J.; Stockbauer, R. *Int. J. Mass Spectrom. Ion Phys.* **1980**, *33*, 243.

(4) The high proton affinity of C_3 precludes proton transfer as a competing channel with many neutral substrates while the high energy of $:C_3H^+$ ensures exoergicity for other reaction channels that can be more revealing of close-range chemical interactions. When exoergic, proton transfer often overrides other reaction channels.

(5) The SIFT apparatus has been described in detail by: Mackay, G. I.; Vlachos, G. D.; Bohme, D. K.; Schiff, H. I. *Int. J. Mass Spectrom. Ion Phys.* **1980**, *36*, 259. In the present experiments C_3H^+ was generated from propene either in the miniature flowing afterglow source in a He buffer at 0.3 torr or from the pure gas at much lower pressures in an axial electron-impact ionizer at an electron energy of 45 eV. After formation the C_3H^+ was selected and injected at ca. 80 V or ca. 8 V, respectively, into a helium carrier gas at total pressures of ca. 0.35 torr. The ions were allowed to thermalize by collisions with the carrier gas prior to their entry into the reaction region. The results were independent of the ion source employed. All measurements were carried out at 296 ± 2 K.

(6) See, for example: Stang, P. J. *Chem. Rev.* **1978**, *78*, 383.

(7) Isomerization of the linear to the cyclic structure requires a 1,2 hydride shift and is likely to involve an activation energy, but the available excess energy should be more than sufficient to meet this energy requirement (as is the case for $C_3H^+ + H_2 \rightarrow C_3H_3^+$). The reaction may also be viewed to occur more directly by side-on attack to form an apparent (2 + 2) electrocyclic intermediate. However this mechanism may be partly forbidden by orbital symmetry rules and so seems less attractive than the mechanism involving true carbenoid insertion.

(8) Pasternack, L.; Nelson, H. H.; McDonald, J. R. *J. Chem. Educ.* **1982**, *59*, 459.

Practically all of the observations reported in Table I can be accounted for in terms of carbene character associated with C_3H^+. Therefore it would appear that after the long-range ion–molecule interaction has brought the species within "chemical range", it is primarily the carbenoid feature of $:C_3H^+$ rather than the delocalized positive charge that determines the path of reaction. Further insight into such behavior should be forthcoming from studies of the reactivities of other possible carbene cations such as $:C_5H^+$, $:C_2N^+$, $:C_4N^+$, and so on. The gas-phase approach with the SIFT technique adopted here is sufficiently versatile to allow such studies and therefore should provide a new opportunity to improve our understanding of carbene chemistry in general.

Acknowledgment. We thank the Natural Sciences and Engineering Council of Canada for financial support.

Registry No. C_3H^+, 75104-46-0; H_2, 1333-74-0; CO, 630-08-0; H_2O, 7732-18-5; H_2S, 7783-06-4; CO_2, 124-38-9; CH_4, 74-82-8; CH_3OH, 67-56-1; C_2H_4, 74-85-1; oxygen, 7782-44-7; cyclopropenylium, 26810-74-2; propylene, 115-07-1.

Nuclear Overhauser Effect Measurements Involving the Imino Protons of Yeast tRNA^{Phe} Using Two-Dimensional Proton NMR Spectroscopy

C. A. G. Haasnoot,* A. Heerschap, and C. W. Hilbers

Department of Biophysical Chemistry, Faculty of Science University of Nijmegen, Toernooiveld 6525 ED Nijmegen, The Netherlands

Received February 22, 1983

The potential of nuclear magnetic resonance (NMR) for structural studies of biomacromolecules greatly depends on the possibility to identify individual resonances in the spectrum. Recently, significant progress has been made in this field, particularly by the systematic application of the nuclear Overhauser effect (NOE). Using so-called one-dimensional NOE techniques, two groups[1,2] have now independently obtained a complete assignment of the imino proton spectrum of yeast tRNA^{Phe}, while part of the imino proton spectra of three other tRNAs have been characterized.[3-5]

Notwithstanding these accomplishments, in principle two-dimensional NOE is a more powerful and more efficient method for the detection of NOE's between neighboring protons in biological macromolecules.[6] Moreover, it has been shown[7] that the 2D-NOE experiment provides an immediate qualitative view of the relative rate of exchange of the imino protons in nucleic acid fragments, i.e., a fingerprint of the stability of individual base pairs in a double helical fragment.

However, in the case of a 2D-NOE experiment involving imino protons, e.g., of yeast tRNA^{Phe}, a serious technical problem is posed by the fact that the imino proton resonances are only detectable when the compound is dissolved in (nondeuterated) water. This experimental condition implies a "dynamic range" problem of a factor 10^5 as the solute signal (typically present in 1 mM concentration) is to be recorded in the presence of a huge water signal (proton concentration ca. 110 M). When imino protons of nucleic acids are involved, the "standard" water suppression technique, i.e., (pre-) irradiation of the solvent signal, is prohibited as chemical exchange between water protons and imino protons will give rise to magnetization transfer from the irradiated water to the nucleic acid imino protons, thus leading to a saturation of the latter resonances and impairing their observation.[8]

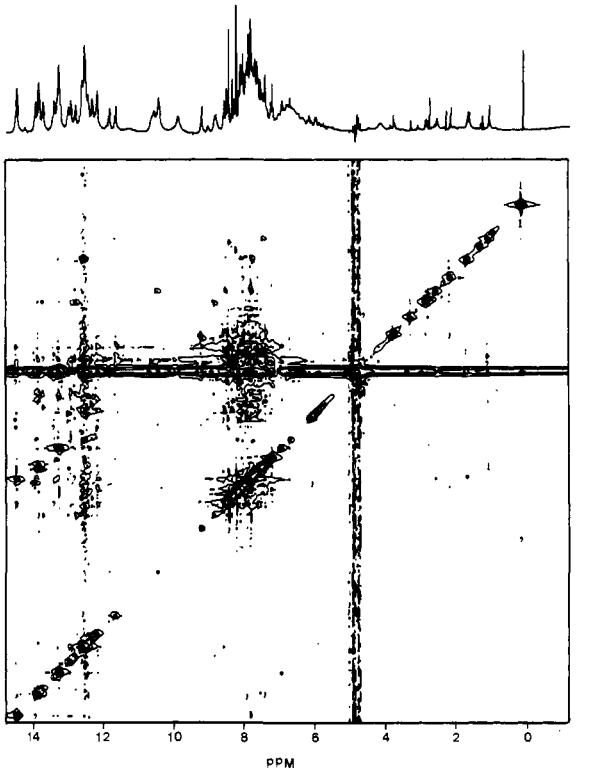

Figure 1. Contour plot of a 500-MHz ^1H NMR 2D-NOE spectrum of yeast tRNA^{Phe} (1.8 mM dialyzed against H_2O/D_2O, 95:5 v/v, containing 5 mM $MgCl_2$, 0.1 mM EDTA, and 12 mM Na_2HPO_4, pH 6.9), T = 28 °C. Spectral width was 20 000 Hz; quadrature detection was used with the carrier at the low-field end of the spectrum. The data set consisted of 4K data points in ω_1-dimension, 512 data points in ω_2-dimension; 256 FID's were accumulated for each value of t_1; total acquisition time was ca. 66 h. Before Fourier transformation, the FID's were multiplied with a sine-bell window[11] and zero filled to 2K data points in the ω_1-dimension. An absolute value plot of the relevant part of the spectrum is shown. The nonsymmetrical appearance of the contour plot is a result of the method of data collection and processing.[7] The vertical and (partly) the horizontal spikes at 4.75 ppm are due to the resonance of residual solvent protons. The top spectrum is a normal 1D spectrum of the same sample recorded by using a time-shared long pulse in combination with DSA.[7] Total accumulation time 6 min, no digital filtering was applied before Fourier transformation.

Recently, an alternative experimental method using a semiselective observation pulse in combination with the digital shift accumulation (DSA) technique was proposed[7] for the present type of measurements. Moreover, it was shown[7] that the method is easily extended to 2D-NOE experiments. Backed by this water suppression technique we explored the limits of 2D-NOE NMR spectroscopy and report here a 2D-NOE experiment involving the imino protons of yeast tRNA^{Phe}. It will be shown that 2D-NOE spectroscopy is indeed feasible for a molecule of the size of a tRNA (molecular weight ~28 000).

Figure 1 shows the absolute value contour plot of the 2D-NOE spectrum of a 1.8 mM solution of tRNA^{Phe}. The spectrum was recorded by using the $[90°-t_1-90°-\tau_m-90°-\text{Acq}(t_2)]$ pulse sequence introduced by Macura and Ernst[9] except that in our experiment the last pulse (the observation pulse) was replaced by a time-shared long pulse.[7] The mixing time τ_m was 0.3 s. After recording the spectra, the FID's were subjected to a DSA treatment,[10] followed by window multiplication and Fourier transformation in two dimensions. For reference purposes a normal 1D spectrum (recorded using a time-shared long pulse in

(1) Heerschap, a.; Haasnoot, C. A. G.; Hilbers, C. W. *Nucl. Acids Res.* **1982**, *10*, 6981–7000; and in press.
(2) Roy, S.; Redfield, A. G. *Biochemistry* **1983**, *22*, 1386–1390.
(3) Hare, D. R.; Reid, B. R. *Biochemistry* **1982**, *21*, 1835–1842.
(4) Hare, D. R.; Reid, B. R. *Biochemistry* **1982**, *21*, 5129–5135.
(5) Roy, S.; Papastravos, M. Z.; Redfield, A. G. *Biochemistry* **1982**, *21*, 6081–6088.
(6) (a) Wuetrich, K.; Wider, G.; Wagner, G.; Braun, W. *J. Mol. Biol.* **1982**, *155*, 311–319. (b) Billeter, M.; Braun, W.; Wuetrich, K. *Ibid.* **1982**, *155*, 321–346. (c) Wagner, G.; Wuetrich, K. *Ibid.* **1982**, *155*, 347–366. (d) Wider, G.; Lee, K. H.; Wuetrich, K. *Ibid.* **1982**, *155*, 367–388.
(7) Haasnoot, C. A. G.; Hilbers, C. W. *Biopolymers* **1983**, *22*, 1259–1266.
(8) Johnston, P. D.; Redfield, A. G. *Nucl. Acids Res.* **1977**, *4*, 3599–3616.
(9) Macura, S.; Ernst, R. R. *Mol. Phys.* **1980**, *41*, 95–117.
(10) Roth, K.; Kimber, B. J.; Feeney, J. *J. Magn. Reson.* **1980**, *41*, 302–309.

0002-7863/83/1505-5483$01.50/0